

Short Communication

Hollow Sphere c-In₂O₃ for Application in Lithium Ion Battery

Xinghua Liang^{1,*}, Qingqing Song¹, Lin Shi¹, Yusi Liu², Gongqin Yan¹, Anbang Jiang¹

¹Guangxi Key Laboratory of Automobile Components and Vehicle Technology, Guangxi University of Science and Technology, Guangxi, Liuzhou 545600, China; ²Shanghai Jiao Tong University, Shanghai 200240, China

*E-mail: lxh304@aliyun.com,

Received: 23 March 2015 / Accepted: 18 April 2015 / Published: 28 April 2015

The hollow sphere c-In₂O₃ were synthesized via hydrothermal reaction. The crystal structure of the sample was collected and analyzed through X-ray diffractometry (XRD). The surface morphology and particle size of the sample were observed by scanning electron microscope (SEM). The electrochemical property of the hollow sphere c-In₂O₃ as cathode for Li-ion Batteries were studied. Hollow Sphere c-In₂O₃ shows a discharge capacity was 1162 mAh·g⁻¹ at the current density of 30 mA·g⁻¹ in a voltage of 0.2-1.4V, and the reversible capacity is around 100 mAh·g⁻¹ after 40 cycles.

Keywords: c-In₂O₃; hydrothermal; hollow sphere; metal oxide; lithium ion battery

1. INTRODUCTION

In recent years, growing demands in various electronic devices, digital communication, hybrid electric vehicles, other related devices, and high power source have been investigated[1]. As new potential anode of materials rechargeable lithium batteries, metal oxides been applied to the area of the energy storage [2,3]. Due to unique physical, chemical properties [4], and higher theoretical reversible capacity (500~1000 mAh·g⁻¹), metal oxides than that of the current commercial graphite (~370mAh·g⁻¹)[5-8].

Hollow sphere of metal oxides have been attended for several years, because of their unique properties of specific structural, nanometer sizes, good permeation, low density, and high specific surface area [7]. Many methods have been developed to fabricate hollow sphere of metal oxides, for instance, pyrohydrolytic [9], hydrothermal method [10-15], thermal evaporation [16], chemical vapor deposition [17], pulsed laser deposition [2,18] and electrochemical deposition [18].

Indium oxide (In_2O_3) as promising cathode material has been attracted attention, owing to its high theoretical capacities, electrical conductivity and applications extensively [19-20]. In_2O_3 is very important n-type semiconductor binary oxide with direct band gap of 3.55-3.75eV and indirect band gap around 2.8 eV, and has been widely applied in microelectronic areas including gas sensors, transparent conductors, solar cells, ultrasensitive toxic gas detectors, and liquid crystal display devices [9,10,21,22]. In_2O_3 has three different crystal structures: cubic bixbyite-type (c- In_2O_3), hexagonal corundum-type (h- In_2O_3) and orthorhombic Rh_2O_3 (II)-type[23]. c- In_2O_3 is stable under ambient conditions and the last structure is stable only under high pressures and temperatures [3,4,11].

In this work, we demonstrate a facile hydrothermal process for controllable synthesis of hollow sphere c- In_2O_3 . The crystal structure and morphology of samples are observed through X-ray diffraction (XRD) and scanning electron micrographs (SEM). Moreover, the electrochemical properties of the hollow sphere c- In_2O_3 have been investigated as cathode materials for Li-ion Batteries. The results show that the as-prepared hollow sphere c- In_2O_3 exhibit high discharge capacity and coulombic efficiency.

2. EXPERIMENTAL METHODS

The hollow sphere c- In_2O_3 sample was synthesized by hydrothermal process: 0.381g $\text{In}(\text{NO}_3)_3 \cdot 4.5\text{H}_2\text{O}$ and 8g sucrose were dissolved in 30 mL distilled water. 1 mL of dimethylformamide was added into the former liquor under vigorous stirring for 1h, at room temperature. The resulting mixture was transferred into a Teflon-lined stainless steel autoclave of 50 mL capacity. The autoclave was then sealed and maintained at 80°C for 20h in an oven followed by cooling the autoclave down to room temperature naturally. After being cooled, the prepared white precipitate was collected by centrifugation and washed with distilled water and the absolute ethanol. The washing cycle was repeated several times, followed by drying at 80°C overnight. The product was white $\text{In}(\text{OH})_3$ sample. Finally, the yellow hollow sphere c- In_2O_3 sample was obtained from the white $\text{In}(\text{OH})_3$ sample via calcination at 550°C for 2h with heating rate of 2°C·min⁻¹, and cooling rate of 1°C·min⁻¹, in a muffle furnace.

The crystalline phase of In_2O_3 was identified by an X-ray diffractometer (Bruker D8 Advance) using Cu K α radiation ($\lambda=0.154184$ nm) with 40 kV of voltage and 30 mA of current. XRD data was recorded at 2 θ with a step size of 0.03° in the range from 10° to 90°. The particle size and morphology of hollow sphere c- In_2O_3 powders were observed with a scanning electron microscope.

The electrochemical performance of the hollow sphere c- In_2O_3 powders as cathode was evaluated using a CR2016 coin-type cell with a lithium metal anode. The CR2016 coin-type cell was fabricated with the hollow sphere c- In_2O_3 cathode, a metallic lithium anode, and a Celgard polypropylene separator. The electrolyte solution was 1M LiPF₆ / DOL+DMC (1:1). The electrode was prepared by mixing 80 wt.% the hollow sphere c- In_2O_3 sample with 10 wt.% acetylene black and 10 wt.% polypropylene fluoride (PVDF) binder in N-methylpyrrolidone (NMP) to form a slurry. The slurry was stirred 4h, then coated onto a copper foil, and dried at 120°C for 12h in a vacuum drier to prepare the cathode film. The cathode film was punched into discs (diameter=14mm). The cell was

fabricated in an Ar-filled glove box. The assembled cell was charged and discharged between 0.2V and 1.4V (versus Li/Li⁺) on the a multi-channel battery test system instrument at room temperature.

3. RESULTS AND DISCUSSION

Fig.1 shows a full set of diffraction peaks of the In₂O₃ sample. The sharp peaks in the pattern showed good crystallinity of the In₂O₃ sample. It is seen that a few of strong peaks at the near 21.49°, 30.58°, 35.47°, 51.04°, 83.20° can be indexed to the cubic phase of c-In₂O₃ (JCPDS no.06-0416), which is invisible in the XRD patterns[11]. The lattice parameters refined within this space group for the new phase are a=1.012nm (a=1.0118nm from JCPDS no.06-0416), and unit cell volume V₀=0.065 nm³.

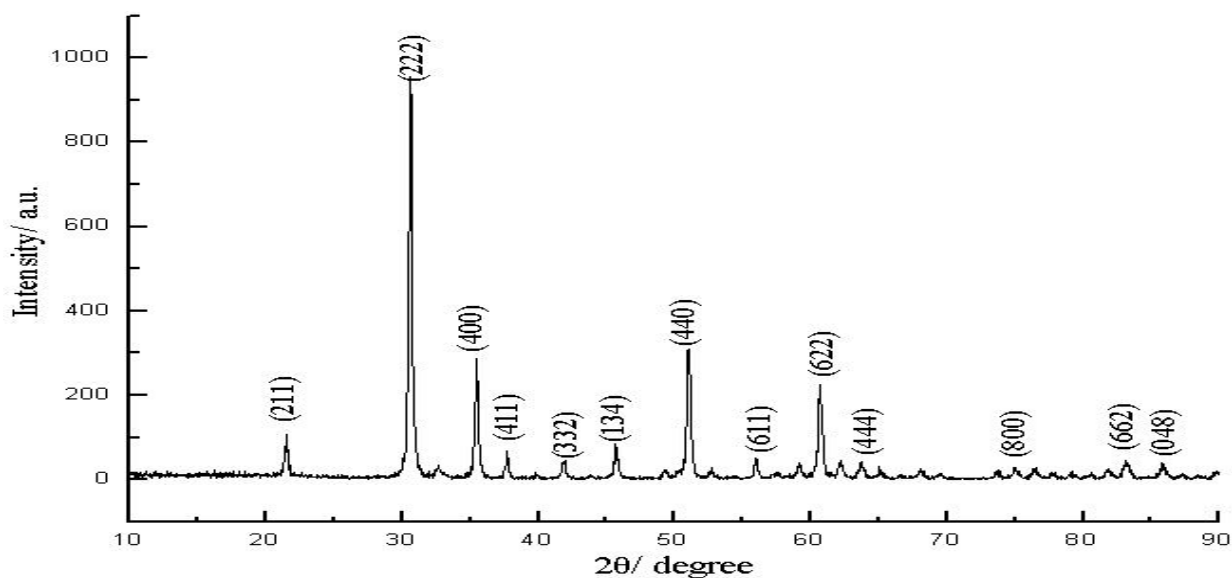


Figure 1. XRD pattern of hollow sphere c-In₂O₃

In Fig.2, it vividly reveals that the In₂O₃ sample consists of hollow sphere microspheres and sphere-section with a diameter of about 1-3μm. More interestingly, both the inner and outer surface of the hollow c-In₂O₃ sample are rough (Fig.2 a,b). The thickness of the hollow ball is about 0.6μm. It worth noting that some of the hollow ball is incomplete. Sphere wall was structure by nanocrystals (Fig.2 c). It is well-known that rate capability plays an important role in lithium ion battery. The electrochemical performance of hollow sphere c-In₂O₃ were evaluated by galvanostatic measurements. Fig.3 shows that the first discharge curve of the coin cell between 0.2V and 1.4V, at a constant current density of 30 mA·g⁻¹.

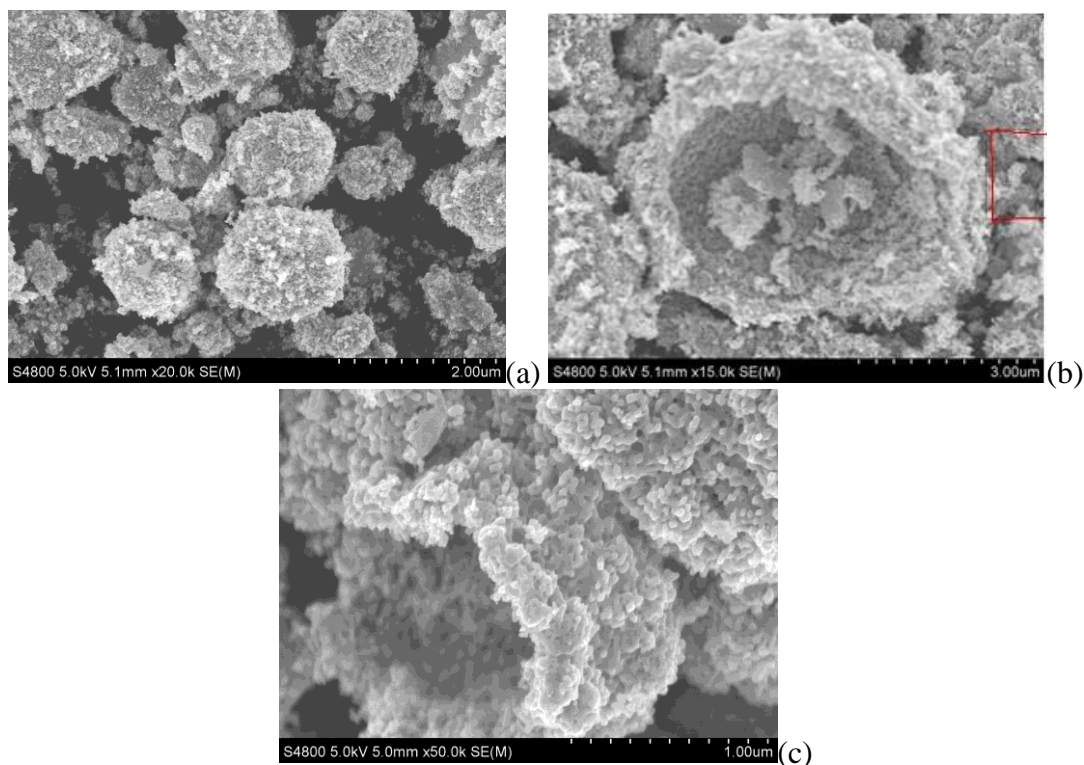


Figure 2. (a) (b) SEM image of hollow sphere c-In₂O₃; (c) magnified SEM image of hollow sphere c-In₂O₃ nanoparticles of the position marked in (b).

In the initial discharging process, there is a long smooth voltage plateaus around 0.9V, and The first discharge capacity is 1162 which is higher than that report by Zhou et al[2]. However, with the increase of the cycling times, the discharge capacity of the coin cell presents a downward trend. Especially, the second discharge capacity downs quickly from 1162 mAh·g⁻¹ to 201 mAh·g⁻¹. After the five cycle, the discharge capacity curve of the coin cell keeps a stable condition.

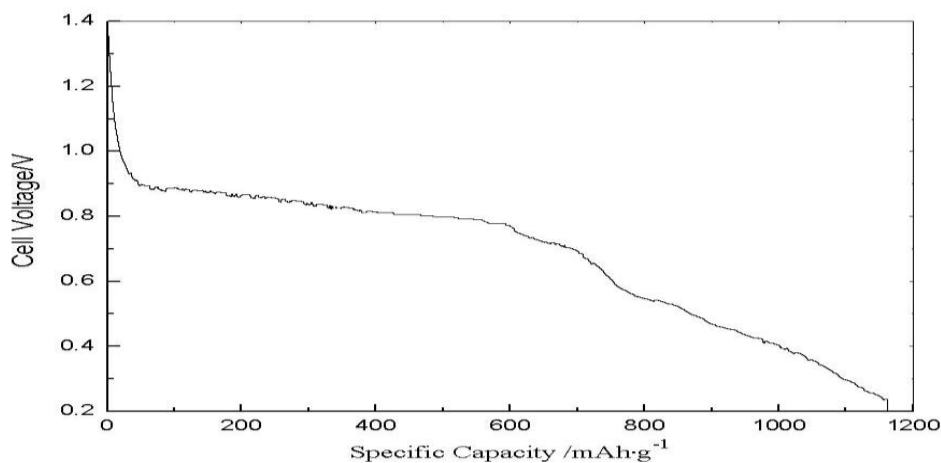


Figure 3. The first discharge curve of the Li/In₂O₃ coin cell

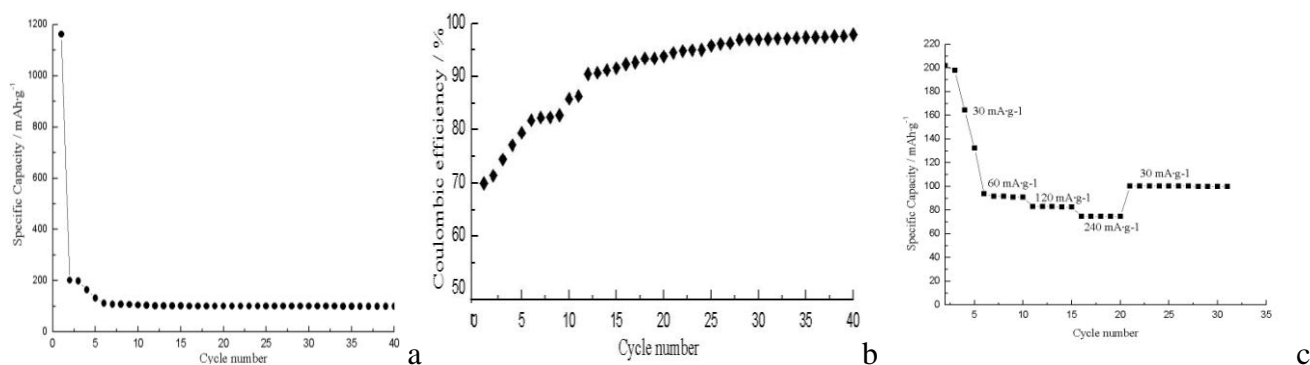


Figure 4. Electrochemical properties of hollow sphere $c\text{-In}_2\text{O}_3$: (a) specific capacity of $\text{Li}/\text{In}_2\text{O}_3$ coin cell; (b) coulombic efficiency of $\text{Li}/\text{In}_2\text{O}_3$ coin cell; (c) rate performance of $\text{Li}/\text{In}_2\text{O}_3$ coin cell

It suggests that hollow sphere $c\text{-In}_2\text{O}_3$ has large irreversible capacity. In the 40th cycle, the discharge capacity of the coin cell only remains about $100 \text{ mAh}\cdot\text{g}^{-1}$ (Fig. 4a). The massive capacity reduction may be attributed to lithiation reaction initially and delithiation of the electrode in the lithium ion battery [5]. Coulombic efficiency is a key index for evaluating the stability of the coin cell. It can be seen that the coulombic efficiency in the first cycle is low and unstable, and becomes gradually increasing from 70% to 94% (Fig. 4b), which may be due to the diffusion rate of Li^+ ions in hollow sphere $c\text{-In}_2\text{O}_3$ becoming stable. As shown in Fig. 3c, it can be seen that the discharge capacity of the coin cell decreased quickly at the current density of $30 \text{ mA}\cdot\text{g}^{-1}$ during the first five cycles. When the current density gradually increased from $60 \text{ mA}\cdot\text{g}^{-1}$ to $240 \text{ mA}\cdot\text{g}^{-1}$, the In_2O_3 electrode delivered a capacity of $90 \text{ mAh}\cdot\text{g}^{-1}$, $82 \text{ mAh}\cdot\text{g}^{-1}$, $74 \text{ mAh}\cdot\text{g}^{-1}$, respectively. While the current density back to $30 \text{ mA}\cdot\text{g}^{-1}$ after being continuously cycled for 10 times, a capacity of $101 \text{ mAh}\cdot\text{g}^{-1}$ can be obtained, indicating good robustness and stability of hollow sphere $c\text{-In}_2\text{O}_3$ material.

4. CONCLUSION

In conclusion, the hollow sphere $c\text{-In}_2\text{O}_3$ sample was prepared by hydrothermal method. According to the XRD and SEM, sample was cubic bixbyite-type structure (Ia-3) In_2O_3 , good crystallinity and hollow sphere. The sample presented the large discharge capacity of $1162 \text{ mAh}\cdot\text{g}^{-1}$ at the current density of $30 \text{ mA}\cdot\text{g}^{-1}$ between 0.2V and 1.4V. The discharge capacity faded quickly in the charge-discharge process. After 40 cycles, the reversible capacity was around $100 \text{ mAh}\cdot\text{g}^{-1}$, and coulombic efficiency rises to 94%.

ACKNOWLEDGEMENTS

This work was financially supported by the Building Fund (No.13-051-38) and Opening Project of Guangxi Key Laboratory of Automobile Components and Vehicle Technology (No.2012KFMS04, 2013KFMS01).

References

1. K.R. Prasad, K. Koga and N. Miura, *Chem. Mater*, 16 (2014) 1845.
2. Y.N. Zhou, H. Zhang, M.Z. Xue, C.L. Wu, X.J. Wu and Z.W. Fu, *J. Power Sources*, 162 (2006) 1373.
3. D. Liu, W.W. Lei, S. Qin and Y. Chen, *Electrochim Acta*, 135 (2014) 128.
4. D. Liu, W.W. Lei, S. Qin, L.T. Hou, Z.W. Liu, Q.L. Cui and Y. Chen, *J Mater Chem A* , 1 (2013) 5274.
5. L. Zhao, W.B. Yue and Y. Ren, *Electrochim Acta* , 116 (2014) 31.
6. S. Qin, W.W. Lei, D. Liu, P. Lamb and Y. Chen, *Mater Lett*, 91 (2013) 5.
7. H. Li, X.J. Huang and L.Q. Chen, *Solid State Ionics*, 123 (1999) 189.
8. X.H. Huang, J.P. Tu, B. Zhang, C.Q. Zhang, Y. Li, Y.F. Yuan, et al. *J. Power Sources*, 161 (2006) 541.
9. W.H. Zhang and W.D. Zhang, *J Solid State Chem*, 186 (2012) 29.
10. B.X. Li, Y. Xie, M. Jing, G.X. Rong, Y.C. Tang and G.Z. Zhang, *Langmuir*, 22 (2006) 9380.
11. H.X. Yang, L. Liu, H. Liang, J.J. Wei and Y.Z. Yang, *CrystEngComm*, 13 (2011) 5011.
12. X. He, H.R. Liu, H.L. Dong, J. Liang, H. Zhang and B.S. Xu, *J Inorg Mater*, 29 (2014) 264.
13. X. Yang, J. Xu, T.L. Wong, Q.D. Yang and C.S. Lee, *Phys Chem Chem Phys*, 15 (2013) 12688.
14. M.M. Titirici, M. Antonietti and A. Thomas, *Chem Mater*, 18 (2006) 3808.
15. J. Yang, C.K. Lin, Z.L. Wang and J. Lin, *Inorg Chem*, 45 (2006) 8973.
16. M.A. Mahdi, J.J. Hassan, S.J. Kasim, S.S. Ng and Z. Hassan, *Mat Sci Semicon Proc*, 26 (2014) 87.
17. Q.Y. Wang, K. Yu, F. Xu, J. Wu, Y. Xu and Z.Q. Zhu, *Mater Lett*, 62 (2008) 2710.
18. T.G. Kim, H.B. Oh, H. Ryu and W.J. Lee, *J Alloy Compd*, 612 (2014) 74.
19. R. Yang, J. Zheng, J. Huang, X.Z. Zhang, J.L. Qu and X.G. Li, *Electrochem Commun*, 12 (2010) 784.
20. W.H. Ho, C.F. Li, H.C. Liu and S.K. Yen, *J. Power Sources*, 175 (2008) 897.
21. Y.W. Hu, W. Zhang and W. Pan, *Mater Res Bull*, 48 (2013) 668.
22. Z.M. Li, P.Y. Zhang, T. Shao and X.Y. Li, *Appl Catal B-Environ*, 125 (2012) 350.
23. D. Liu, W. W. Lei, B. Zou, S. D. Yu, J. Hao, K. Wang, B. B. Liu, Q. L. Cui and G. T. Zou, *J. Appl. Phys.*, 104 (2008) 083506.